Neuroscience Letters 482 (2010) 95–100

Contents lists available at ScienceDirect

Neuroscience Letters

journal homepage: www.elsevier.com/locate/neulet

Investigation of acupoint specificity by functional connectivity analysis based on graph theory

Yanshuang Ren[a,b], Lijun Bai[c], Yuanyuan Feng[c], Jie Tian[c,*], Kuncheng Li[a,**]

[a] Department of Radiology, Xuanwu Hospital, Capital Medical University, Changchun Street No. 45, Xuan Wu District, Beijing 100053, China
[b] Department of Radiology, Guanganmen Hospital, Chinese Academy of Traditional Medicine, Beijing 100053, China
[c] Medical Image Processing Group, Institute of Automation, Chinese Academy of Sciences, Zhong Guancun East Rd. No. 95, Beijing 100190, China

ARTICLE INFO

Article history:
Received 17 May 2010
Received in revised form 23 June 2010
Accepted 29 June 2010

Keywords:
Acupuncture
Acupoint specificity
Graph theory
Functional magnetic resonance imaging (fMRI)

ABSTRACT

Acupoint specificity is still a contentious issue and remains to be verified whether brain, response is as specific as the purported indication of different acupoints. Previous fMRI acupuncture, studies based on multiple-block design may not be able to fully disclose acupuncture effects. Both, recent studies and certain clinical reports have indicated that there exists time-sustainability during, acupuncture even after the stimulus being terminated. Further understanding of how such external, intervention interacts with post-stimulus resting brain networks may enlighten us to gain an, appreciation of the physiological function and integrated mechanisms involved in acupuncture. In our, study, we adopted a modified non-repeated event-related (NRER) design, and utilized the graph theory, based functional connectivity analysis to investigate the neural specificity of the PC6, with the same, meridian acupoint PC7 and a different meridian acupoint GB37 as separate controls. Under the, construct of this network model, some brain regions with a larger degree of connectivity indicated, stronger interactions with other brain regions and were considered to be important nodes in this, network. We identified that the two most important brain areas were the right nodule and right uvula, following acupuncture at PC6, and the right amygdala and right inferior parietal lobe following, acupuncture at PC7. Following the GB37, the two regions with the larger degree of connectivity were, the posterior cingulate cortex (PCC) and middle occipital gyrus. These specific regions may mediate the, specific effects of acupuncture. Results showed that different modulatory brain networks may support, the point specificity of acupuncture.

Acupuncture is an ancient East Asian healing modality that has been in use for more than 2000 years. Acupoint specificity lies at the core of traditional acupuncture theory. The traditional point that has received most supports from controlled trials is probably PC6 for nausea [16]. Whether brain response is as specific as the purported indications of different acupoints remains to be verified.

Previous fMRI acupuncture studies based on multiple-block design may not be able to fully disclose acupuncture effects. Certain clinical reports have indicated that the therapeutic effects of acupuncture can last several minutes, even longer. For example, the analgesic effects of acupuncture may actually peak long after cessation of active needle stimulation [23]. One recent study has indicated that there exists time-variability and long-lasting effects during the course of multiple-block acupuncture [4]. Therefore, imaging its sustained effect on the brain networks may further help elucidate the mechanisms by which acupuncture achieves its therapeutic effects [3]. In our study, a new experimental paradigm, namely the non-repeated event-related fMRI (NRER-fMRI) design, was implemented.

Previous studies have defined low-frequency, spatially consistent networks in resting fMRI data which may reflect the functional connectivity [7,8,11,18]. To investigate the sustained effects of acupuncture, Dhond et al. used the probabilistic independent component analysis (pICA) to evaluate acupuncture modulation of functional connectivity within resting state networks (RSNs). The results demonstrate that acupuncture can enhance the post-stimulation spatial extent of RSNs underlying the anti-nociceptive, memory and affective processing [9]. Another research also indicates that acupuncture can further enhance the dichotomy of anticorrelated resting brain networks and modulate intrinsic coherences within the "salience" network (SN), including the paralimbic regions and brainstem nuclei [5]. This modulation may relate to acupuncture analgesia and other potential therapeutic effects. However, these investigations have only explored the spatial distribution of neural response to acupuncture, and may ignore the critical issue of which brain regions implicated in the network are more important. In our study, we adopted a graph theory

* Corresponding author. Tel.: +86 010 62527995; fax: +86 010 62527995.
** Corresponding author. Tel.: +86 010 83198376; fax: +86 010 83198376.
E-mail addresses: tian@ieee.org (J. Tian), likuncheng1955@yahoo.com.cn (K. Li).

0304-3940/$ – see front matter.
doi:10.1016/j.neulet.2010.06.091

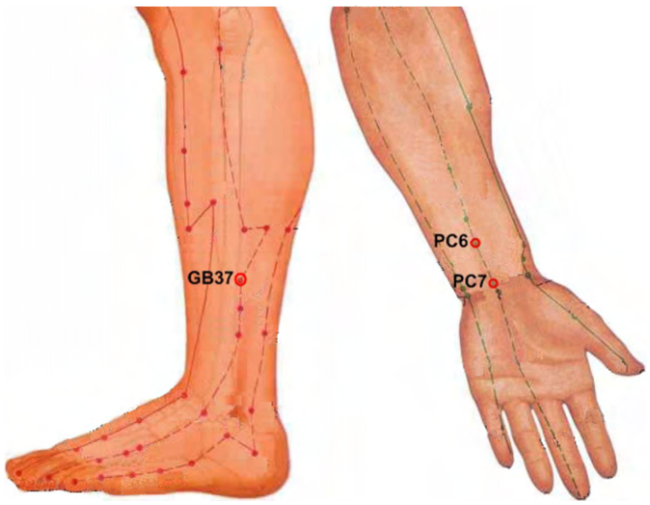

Fig. 1. Illustration of anatomical locations of three acupoints: PC6 (Neiguan), PC7 (Daling) and GB37 (Guangming).

based network model to describe the functional connectivity in the post-acupuncture resting state [15]. We used connectivity degrees to quantify the importance of nuclei implicated in the network. Some brain regions with a larger degree of connectivity indicated stronger interactions with other brain regions and were considered to be important nodes in this network. We speculated these specific brain regions may be underlying the specific effects of acupuncture.

According to Traditional Chinese Medicine, acupuncture at specific acupoints is able to treat certain types of diseases [6]. In this study, we investigated if some specific brain regions during post-stimulation were related to the existence of point specificity of acupuncture among pericardium 6 (PC6) (Neiguan, an important acupoint for preventing nausea and vomiting), gallbladder 37 (GB37) (Guangming, located at different meridian serving as treatments for multiple vision-related disorders) and pericardium 7 (PC7) (Daling, belonging to the same meridian and median innervation with PC6 as indications for depressive psychosis and palpitation). By detecting different modulatory brain networks underlying the same meridian and different meridian acupoints, we provided further evidence to test the point specificity of acupuncture and promote its acceptance as a viable clinical treatment.

Participants in the fMRI experiments were recruited from a homogeneous group of 36 college students (18 males, ages of 21.4 ± 1.3), claiming to be in good health with no history of neurological illness. Subjects were all acupuncture naïve, and right-handed according to the Edinburgh Handedness Inventory [22]. On commencing the study, an envelope method was used to allocate subjects to receive once acupuncture at one of the three acupoints in a random sequence, with the gender ratio balanced (ANOVA, $P > 0.6$) among different groups. After a complete description of the study was given to all subjects, written informed consent was obtained, as approved by a local subcommittee on Human Studies.

The NRER-fMRI scanning lasted 4 min/run, including 2 min needling manipulations preceded by a 1 min rest, and followed by another 1 min rest scanning. Acupuncture was performed on three acupoints (shown in Fig. 1): PC6 is located approximately 3 cm above the midpoint of the transverse crease of the wrist, between the tendon of palmaris longus and flexor carpi radialis [25]; PC7 is located at the midpoint of the crease of the wrist, between the tendons of the long palmar muscle and radial flexor muscle [10]; GB37 is located in the lateral aspect of the lower leg, with needle being inserted on the anterior border of the fibula [20]. Acupuncture stimulation was delivered using a sterile disposable 38 gauge stainless steel acupuncture needle, 0.2 mm in diameter and 40 mm in length. The needle administration was delivered by a balanced "tonifying and reducing" technique [12], rotating clockwise and counterclockwise for 1 min at a rate of 60 times per min. Considering the anatomical differences, the needling depth ranged from 0.5–1.0 cm for PC6 and PC7 to 1.5–2.0 cm for GB37. The procedure was performed by the same experienced and licensed acupuncturist. During the experiment, the subjects were requested to keep their eyes closed and remain relaxed without engaging in any mental tasks.

At the end of each fMRI scanning, the subjects completed a questionnaire that used a 10-point visual analogue scale (VAS) to rate their experience (or "deqi") of aching, pressure, soreness, heaviness, fullness, warmth, coolness, numbness, tingling, dull or sharp pain they felt during the scan [13,17]. The VAS was scaled at 0 = no sensation, 1–3 = mild, 4–6 = moderate, 7–8 = strong, 9 = severe and 10 = unbearable sensation. Because sharp pain was considered an inadvertent noxious stimulation, we excluded the subjects from further analysis if they experienced sharp pain (greater than the mean by more than two standard deviations) [13]. Among the 36 participants, none experienced the sharp pain.

The images were acquired on a 3.0 Tesla Signa (GE) MR scanner. Thirty-two axial slices (FOV = 240 mm × 240 mm, matrix = 64 × 64, thickness = 5 mm), parallel to the AC-PC plane and covering the whole brain were obtained using a T2*-weighted single-shot, gradient-recalled echo planar imaging (EPI) sequence (TR = 2000 ms, TE = 30 ms, flip angle = 90°). After the functional run, high-resolution structural information was also acquired using 3D MRI sequences with a voxel size of $1\,mm^3$ for anatomical localization (TR = 2.7 s, TE = 3.39 ms, matrix = 256 × 256, FOV = 256 mm × 256 mm, flip angle = 7°, slice thickness = 1 mm).

All preprocessing steps were carried out using statistical parametric mapping (SPM5, http://www.fil.ion.ucl.ac.uk/spm/). The images were first slice-timed and then realigned to correct for head motions using least-squares minimization (none of the subjects had head movements exceeding 1 mm on any axis and head rotation greater than 1°). A mean image created from the realigned volumes was coregistered with the subject's individual structural T1-weighted volume image. The image data was further processed with spatial normalization based on the MNI space and re-sampled at 2 mm × 2 mm × 2 mm [2]. Finally, the functional images were spatially smoothed with a 6 mm full-width-at-half maximum (FWHM) Gaussian kernel.

Given that the sustained effects of acupuncture may continue into the post-stimulus period, the mean signal intensity of the resting period preceded by the active stimulation served as the baseline. Then the difference in the blood oxygen level-dependent response between stimulus and baseline conditions was estimated at every voxel across the whole brain volume using the general linear model in SPM5. The generated *t*-maps at individual levels were then entered into the "random effect" group analysis framework by the one-sample *t*-test (d.f. = 11) summary statistic ($P < 0.001$, uncorrected). The statistical maps indicated the brain activation in response to acute effects of acupuncture stimuli, thereby functionally defining the regions of interest. The peak voxel and its nearest 10 neighbors were defined as the group interests of region (ROIs). These group ROIs were used to define subject-specific ROIs.

Taking into account the anatomical variability across subjects, subject-specific peak voxels and subject-specific ROIs were defined on individual *t*-maps as follows. A given group ROI was first used as a mask. Then, based on the individual *t*-map, the voxel with the largest *t*-value within this mask was taken as the subject-specific peak voxel. The time courses of voxels within the ROI were averaged to generate a single low-frequency reference time series (node time series for further analysis). ROIs were selected based on the acupuncture stimulation results. In this manner, we obtained a total

of 25 ROI time series related to acupuncture stimulation for each subject.

In this study, we used a network model based on the graph theory to describe the functional connectivity in the post-acupuncture resting brain [15]. The nodes of the network denote the brain regions, and the links describe the connections or information flow among them. In order to measure the connectivity degree η_{ij} between nodes i and j, we used one of the simplest ways which is exponentially related to the distance between them, namely, $\eta_{ij} = \exp(-\xi d_i)$, where ξ is a real positive constant, measuring how the strength of the relationship decreases with the distance between the two nodes (ξ is a subjective selection as discussed by Lopez and Sanjuan [19] and it is here fixed to $\xi = 2$) and d_{ij} is the distance between the two nodes, calculated as a hyperbolic correlation measure. This calculation is as follows: $d_{ij} = (1 - c_{ij})/(1 + c_{ij})$, where c_{ij} represents the Pearson correlation coefficient between the two nodes (that is, cross-correlating two of the averaged time series described above). In this way, we can define the total connectivity degree Γ_i of a node i in a graph as the sum of all the connectivity degrees between node i and all the other nodes, especically, $\Gamma_i = \sum_{j}^{n} 1\eta ij$. This equation describes the amount of information node i receives from the particular network. In this context, a larger Γ means that this region is more functionally connected to other regions in this network. Thus, it is possible to find the changes in the total functional connectivity network by detecting Γ of some specific region under different brain activity states. In this study, as there were different time points and different preprocessing between the three states, we normalized Γ_i of a node i as, $\bar{\Gamma}_i = \Gamma_i / \sum_{j}^{n} = 1\Gamma_j$.

The prevalence of these sensations was expressed as the percentage of individuals in the group that reported the given sensations (Fig. 2). When grouped across all acupoints, no difference was found in regard to the prevalence of the listed sensations elicited by acupuncture stimulation ($P > 0.05$). However, differences did exist with respect to the type of sensations. Soreness and numbness were significantly more frequent for the PC6 than PC7 and GB37 (53% vs. 28% and 33%; 65% vs. 43% and 35%). Fullness and dull pain occurred more commonly for PC7 than PC6 and GB37 (67% vs. 48% and 42%; 67% vs. 25% and 33%). Tingling was saliently more frequent for GB37 (58% vs. 25% and 33%). The average stimulus intensities (mean ± SE) were approximately similar during acupuncture on PC6 (1.85 ± 1.80), PC7 (1.93 ± 2.03) and GB37 (1.83 ± 1.79) under the ANOVA test ($P > 0.05$, Fig. 2). However, soreness was more intense for PC6 than PC7 and GB37 ($P < 0.005$); numbness more intense for PC6 and PC7 than GB37 ($P < 0.005$). Dull pain was stronger for PC7 and GB37 than PC6 ($P < 0.005$), while tingling exhibited more intense for GB 37 than PC6 and PC7 ($P < 0.005$).

The brain regions showed distinct signal changes during acupuncture stimulation at three acupoints. For bilaterally activated regions, we only selected the hemisphere anatomical area with the more significantly t value as the representative ROI. Finally, 25 brain regions were selected as the nodes of the graph further to the connectivity analysis shown in Table 1.

The results of total connectivity degrees for each ROI during the three post-acupuncture resting states were presented in Fig. 3. A larger $\bar{\Gamma}$ suggested that there existed a significant functional connectivity between this brain region and others; thus such region was considered to be an important node in this network. In the case of PC6, the top 10 in $\bar{\Gamma}$ were as follows: the right nodule, right uvula, parahippocampal, right red nucleus, thalamus-ventral posterior lateral nucleus (VPL), right insula, right caudate, right hypothalamus, right culmen, right fastigium. At acupoint PC7, the regions with the 10 highest $\bar{\Gamma}$ values were: the right amygdala, right inferior parietal lobe (IPL), parahippocampal, right red nucleus, thalamus VPL, right caudate, right culmen, left midoccipital, left fusiform gyrus, right fastigium. In the GB37, the more important regions were: the posterior cingulate cortex (PCC), middle occipital gyrus, fusiform gyrus, parahippocampal, red nucleus, thalamus VPL, caudate, culmen, fastigium, middle temporal gyrus.

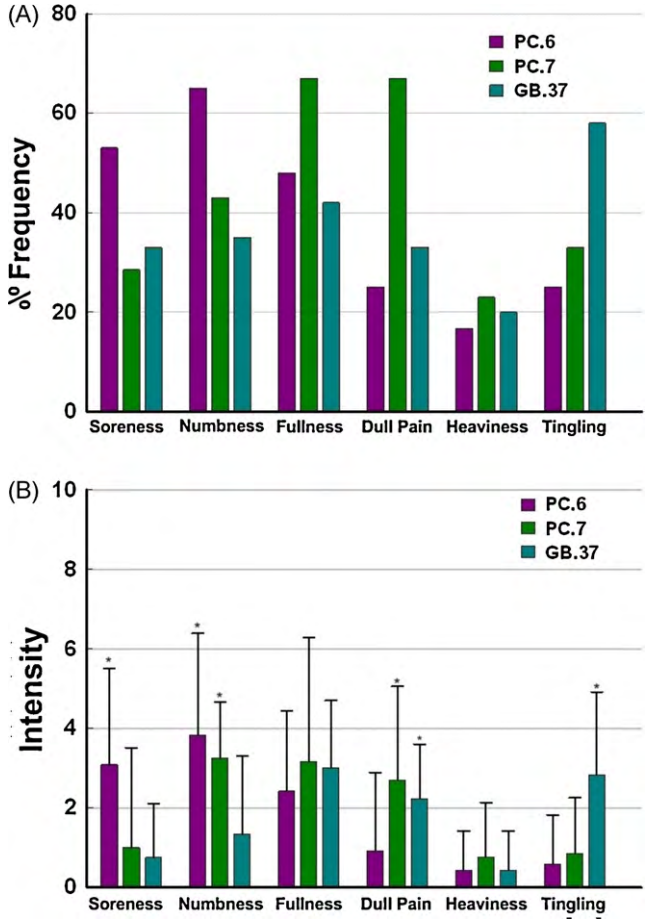

Fig. 2. Averaged psychophysical response ($N = 36$). (A) The percentage of subjects who reported having experienced the given sensation (at least one subject experienced the seven sensations listed). (B) The intensity of reported sensations measured by an average score (with standard error bars) on a scale from 0 denoting no sensation to 10 denoting an unbearable sensation. *Denoting significant differences under Fisher's exact test ($P < 0.005$).

In this paper, we used a graph theory based on the functional connectivity analysis method combining with a new NRER-fMRI design to investigate the specific brain networks following acupuncture stimulation at three different acupoints. Results showed that acupuncture at different acupoints can exert distinct modulatory effects on the reorganizations of functional connectivity of brain networks. Our findings provided preliminary evidence to support the point specificity of acupuncture modulatory effects.

In our study, no difference was found in regard to the psychophysical responses among three different acupoints, and the acupuncture modulatory effects were mainly related to different acupoints. Neuroimaging studies of PC6 during the post-acupuncture resting states were mainly involved the cerebellum related to vestibular functions. Even with the same meridian and the relatively similar treatment usage, following acupuncture at PC7, the more important brain regions were subcortical areas related to affective encoding. Whereas following acupuncture at different meridian acupoint GB37, the more important brain

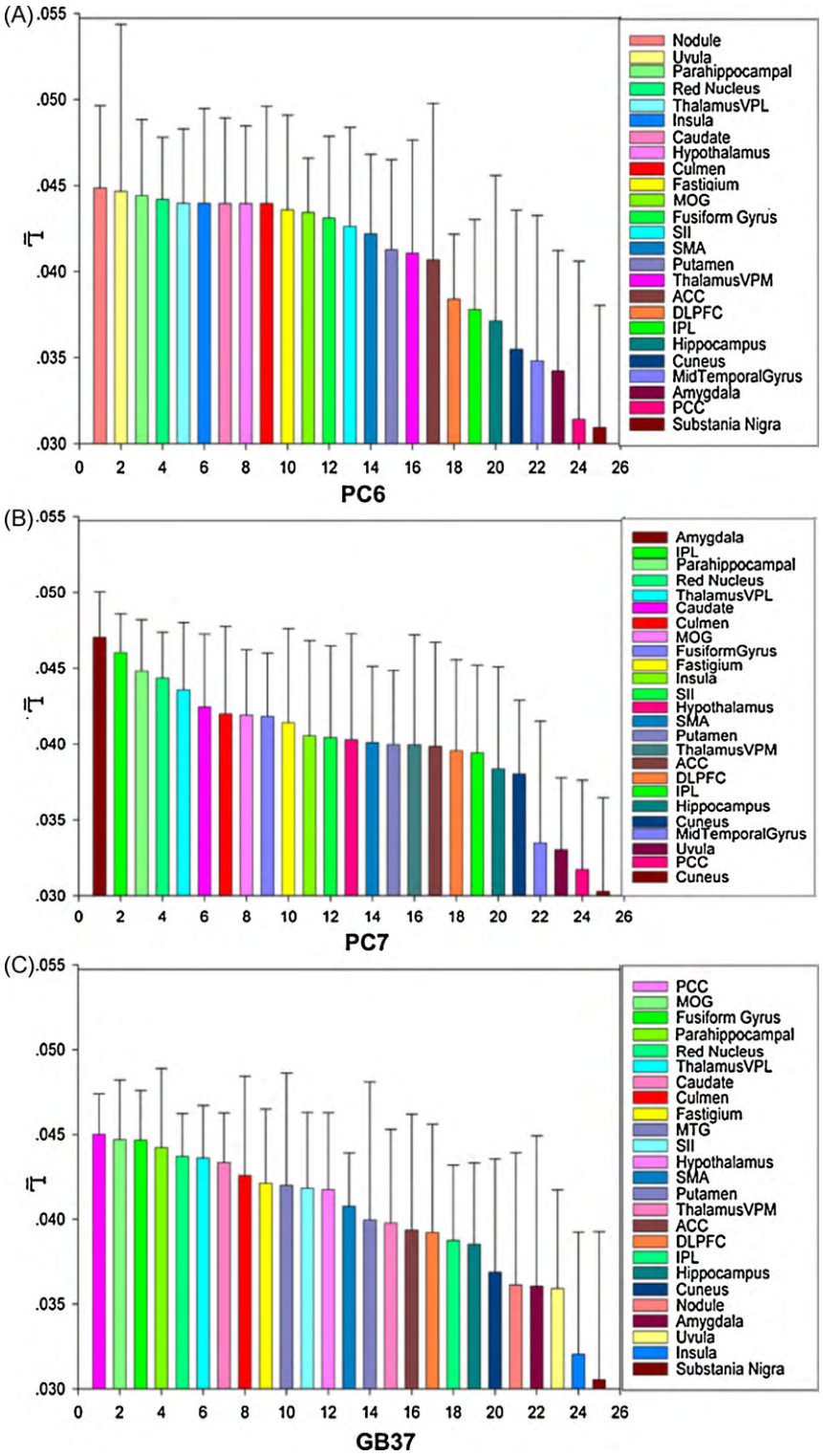

Fig. 3. Ranking of the selected brain regions based on their $\bar{\Gamma}$ (±SD) values across all subjects. The brain regions with larger $\bar{\Gamma}$ values are considered to be important nodes in the resting state of the functional connectivity network. VPL-ventroposterior lateral thalamic nucleus; MOG-middle occipital gyrus; SMA-supplementary motor area; VPM-ventral posterior medial; ACC-anterior cingulate cortex; DLPFC-dorsolateral prefrontal cortex; IPL-inferior parietal lobule; Mid-middle; PCC-posterior cingulate cortex.

regions were mainly comprised of the cortical "association areas", especially the visual cortex.

PC6, an acupoint relevant for the management of nausea including vestibular-related motion sickness [26], has recently been confirmed in abundant clinical trials, such as treating postoperative and chemotherapy nausea and vomiting [21]. In a recent study, acupuncture at PC6 specifically elicited the activation of the cerebellar neuromatrix in comparison with the sham control, thus suggesting a PC6 specific effect that potentially correlates with proven clinical effectiveness [27]. In our study, we identified that the two most important brain areas were the right nodule and right uvula following acupuncture at PC6. The cerebellar uvula-nodulus receives vestibular projections from primary and secondary vestibular afferents, as well as vestibular climbing fibers [1,14,24]. Our

Table 1
. Coordinates and *t* scores of the peak voxel within group ROIs following acupuncture at PC6, PC7 and GB37.

Regions	PC6						PC7						GB37					
		Talairach			*t*	*V*		Talairach			*t*	*V*		Talairach			*t*	*V*
	Hem	*x*	*y*	*z*	Value	Voxels	Hem	*x*	*y*	*z*	Value	Voxels	Hem	*x*	*y*	*z*	Value	Voxels
Fast	R	8	−61	−19	−3.76	21	R	6	−56	−22	−2.73	3	R	6	−48	−19	3.38	8
Cul	R	12	−53	−12	−4.82	413	R	10	−34	−15	−5.20	443	L	−44	−44	−20	4.49	143
Uvula	R	32	−77	−26	4.03	57	L	−6	−71	−27	−3.58	23	R	32	−77	−26	4.03	57
Nodl	R	10	−63	−24	−2.99	22	R	2	−56	−27	−4.02	82	R	2	−56	−27	−4.02	12
Amy	R	22	−4	−12	−4.28	87	L	−18	−8	−11	5.49	51	L	−18	−8	−11	5.49	51
PaHi	L	−26	−53	−6	−2.82	4	L	−12	−37	−2	−4.88	86	L	−22	−33	−2	6.39	33
Hipp	L	−28	−41	4	−2.84	1	L	−28	−35	−3	−2.74	2	L	−28	−14	−11	3.22	15
Insl	R	40	−6	2	−6.68	146	R	42	−38	18	−3.38	34	R	32	−27	11	3.77	20
RedN	R	8	−22	−4	−2.95	4	R	4	−22	−4	−4.96	31	L	−6	−22	−4	3.33	3
SubN	R	12	−22	−7	−3.21	6	R	8	−12	−8	−3.37	14	R	16	−20	−4	5.00	25
Puta	R	28	−16	−6	−3.59	19	L	−24	−11	13	−2.74	1	L	−24	−11	13	6.31	249
VPLL	L	−18	−17	3	−4.31	45	L	−22	−21	8	−2.86	4	L	−18	−19	1	5.08	39
VPML	L	−16	−23	5	5.37	13	L	−16	−21	8	−2.85	3	L	−16	−23	5	5.37	13
Cau	R	22	−34	16	−5.25	17	R	24	−36	13	−3.15	13	L	−32	−33	2	3.38	5
Hypo	L	−8	−6	−3	−2.84	3	L	−8	−6	−3	−2.84	3	L	−8	−6	−3	−2.84	3
Cune	L	−24	−55	−7	−3.43	19	R	16	−88	36	−4.75	40	L	−16	−97	9	3.83	30
FusG	L	−36	−47	−14	−3.77	55	R	−42	−87	−26	−5.37	41	L	−44	−40	−18	5.61	59
MOG	L	−18	−87	17	3.77	16	L	38	−17	6	−3.28	8	L	−18	−87	17	3.77	16
SIIR	R	65	−20	36	−4.54	144	R	67	−19	18	−3.33	5	R	51	−15	54	5.04	53
SMAR	R	61	−17	41	−5.30	20	R	20	−25	53	−3.85	3	L	−51	−4	35	7.91	36
DLPFC	R	57	18	3	−2.68	2	R	57	18	3	−2.68	2	R	59	22	19	4.73	67
IPLR	L	−40	−29	38	−3.42	25	R	65	−42	22	−3.74	14	R	32	−50	54	4.18	5
ACC	L	−20	−16	38	−3.00	3	R	4	11	22	−3.05	4	R	4	11	22	−3.05	4
PCC	L	−46	−42	−15	−2.81	5	R	6	−28	25	−2.95	4	L	−6	−34	22	8.05	17
MTG	L	−65	−29	−4	−4.95	23	L	−65	−29	−4	−4.95	23	R	40	−55	25	5.54	116

Abbreviations: Hem-hemisphere; Fast-fastigium; Cul-culmen; Nodl-nodule; Amy-amygdala; PaHi-parahippocampal gyrus; Hippo-hippocampus; Insl-insula; RedN-red nucleus; SubN-substania nigra; Puta-putamen; VPLL-ventral posterior lateral nucleus; VPML-ventral posterior medial nucleus; Cau-caudate; Hypo-hypothalamus; Cune-cuneus; FusG-fusiform gyrus; MOG-middle occipital gyrus; SII-secondary sensory cortex; SMA-supplementary motor area; DLPFC-dorsolateral prefrontal cortex; IPLR-inferior parietal lobule; ACC-anterior cingulate gyrus; PCC-posterior cingulate; MTG-middle temporal gyrus.

results demonstrated that acupoint PC6 can modulate the specific brain regions relating to vestibular function, subsequently alleviating the symptoms with motion-related sickness and nausea.

Along the same line, acupuncture at PC6 and PC7 has been used clinically to treat mental and psychosomatic disorders [26]. But during post-stimulation state at PC7, the two most important brain areas were exclusively located at the right amygdala and right IPL. The amygdala, located in the medial temporal lobe as part of the limbic system, plays a dominant role in the affective encoding [28]. Acupuncture-related modulation of activity in the amygdala may contribute to stress reduction. GB37 (distinct meridian with respect to PC6 and PC7), an acupoint of the gallbladder channel, which, as its name "brightness" implies, is described as a very effective acupoint influencing multiple vision-related disorders [20]. Our findings demonstrated that the two more important regions following acupuncture at GB37 were located in the PCC and middle occipital gyrus. The PCC, as part of the visual cortex [29], is associated with visuospatial functions, and the occipital lobe mainly supports the vision-related processing [26].

In conclusion, the present study demonstrated the different modulatory brain networks in the post-stimulation state at three different acupoints. Results from our study implied that the therapeutic effects of acupuncture at certain acupoints may depend on the modulation of certain brain areas related to special disorder treatments. But it should be noted that these data were obtained from healthy volunteers receiving one acupuncture treatment, further investigation of these specific therapeutic effects in clinical patients may be needed to verify the findings.

Acknowledgments

This paper is supported by the knowledge innovation program of the Chinese academy of sciences under grant no.KGCX2-YW-129, the Project for the National Key Basic Research and Development Program (973) under Grant no. 2006CB705700, the National Natural Science Foundation of China under Grant nos. 30873462, 30970774, 60901064.

References

[1] A.K. Afifi, R.A. Bergman, Functional Neuroanatomy, Text and Atlas, McGraw-Hill, New York, 1998.
[2] J. Ashburner, K.J. Friston, Nonlinear spatial normalization using basis functions, Hum. Brain Mapp. 7 (1999) 254–266.
[3] L. Bai, W. Qin, J. Tian, P. Liu, L. Li, P. Chen, J. Dai, J.G. Craggs, K.M. von Deneen, Y. Liu, Time-varied characteristics of acupuncture effects in fMRI studies, Hum. Brain Mapp. 30 (2009) 3445–3460.
[4] L. Bai, W. Qin, J. Liang, J. Tian, Y. Liu, Spatiotemporal modulation of central neural pathway underlying acupuncture action: a systematic review, Curr. Med. Imaging Rev. 5 (2009) 167–173.
[5] L. Bai, W. Qin, J. Tian, M. Dong, X. Pan, P. Chen, J. Dai, W. Yang, Y. Liu, Acupuncture modulates spontaneous activities in the anticorrelated resting brain networks, Brain Res. 1279 (2009) 37–49.
[6] S. Beijing, Nanjing Colleges of Traditional Chinese Medicine. Essentials of Chinese Acupuncture, Foreign Language Press, Beijing, 1980, p. 36.
[7] B. Biswal, F.Z. Yetkin, V.M. Haughton, J.S. Hyde, Functional connectivity in the motor cortex of resting human brain using echo-planar MRI, Magn. Reson. Med. 34 (1995) 537–541.
[8] M. De Luca, C.F. Beckmann, N. De Stefano, P.M. Matthews, S.M. Smith, fMRI resting state networks define distinct modes of longdistance interactions in the human brain, Neuroimage 29 (2006) 1359–1367.
[9] R.P. Dhond, C. Yeh, K. Park, N. Kettner, V. Napadow, Acupuncture modulates resting state connectivity in default and sensorimotor brain networks, Pain 136 (2008) 407–418.
[10] J.W. Dundee, W.N. Chestnutt, R.G. Ghaly, A.G. Lynas, Traditional Chinese acupuncture: a potentially useful antiemetic, BMJ 293 (1986) 583–584.
[11] P. Fransson, How default is the default mode of brain function? Further evidence from intrinsic BOLD signal fluctuations, Neuropsychologia 44 (2006) 2836–2845.
[12] K.K.S. Hui, J. Liu, N. Makris, R.L. Gollub, A.J.W. Chen, C.I. Moore, D.N. Kennedy, B.R. Rosen, K.K. Kwong, Acupuncture modulates the limbic system and subcortical gray structures of the human brain: evidence from fMRI studies in normal subjects, Hum. Brain Mapp. 9 (2000) 13–25.
[13] K.K.S. Hui, J. Liu, O. Marina, V. Napadow, C. Haselgrove, K.K. Kwong, D.N. Kennedy, N. Makris, The integrated response of the human cerebro-cerebellar

and limbic systems to acupuncture stimulation at ST36 as evidenced by fMRI, Neuroimage 27 (2005) 479–496.
[14] M. Ito, Neurophysiology of the nodulofloccular system, Rev. Neurol. 149 (1993) 692–697.
[15] T.Z. Jiang, Y. He, Y.F. Zang, X.C. Weng, Modulation of functional connectivity during the resting state and the motor task, Hum. Brain Mapp. 22 (2004) 63–71.
[16] B. Knight, C. Mudge, S. Openshaw, A. White, A. Hart, Effect of acupuncture on nausea of pregnancy: a randomized, controlled trial, Obstet. Gynecol. 97 (2) (2001) 184–188.
[17] J. Kong, R. Gollub, T. Huang, G. Polich, V. Napadow, K. Hui, M. Vangel, B. Rosen, Acupuncture de qi, from qualitative history to quantitative measurement, J. Altern. Complement. Med. 13 (2007) 1059–1070.
[18] M.J. Lowe, B.J. Mock, J.A. Sorenson, Functional connectivity in single and multislice echoplanar imaging using resting-state fluctuations, Neuroimage 7 (1998) 119–132.
[19] L. Lopez, M.A.F. Sanjuan, Relation between structure and size in social networks, Phys Rev E. 65 (2002) 036107.
[20] G.W. Liu, Acupoints of three Yang meridians of foot, in: G.W. Liu (Ed.), Acomplement Work of Present Acupuncture and Moxibustion, Huaxia Publishing House, Tianjin, 1997, pp. 327–479.
[21] NIH, NIH consensus conference statement acupuncture, JAMA 280 (1998) 1518–1524.
[22] R.C. Oldfield, The assessment and analysis of handedness: the Edinburgh inventory, Neuropsychologia 9 (1971) 97–113.
[23] D.D. Price, A. Rai, L.R. Watkins, B. Buckingham, A psychophysical analysis of acupuncture analgesia, Pain 19 (1984) 27–42.
[24] V.E. Pettorossi, S. Grassi, P. Errico, N.H. Barmack, Role of cerebellar nodulus and uvula on the vestibular quick phase spatial constancy, Acta Otolaryngol. 545 (Suppl.) (2001) 155–159.
[25] G. Stux, B. Pomeranz, Acupuncture: Textbook and Atlas, Springer-Verlag, Berlin, 1987, pp. 231–244.
[26] G. Stux, B. Pomeranz, Basics of Acupuncture, Springer-Verlag, Berlin, 1997, pp. 77–92.
[27] S.S. Yoo, E.K. Teh, R.A. Blinder, F.A. Jolesz, Modulation of cerebellar activities by acupuncture stimulation: evidence from fMRI study, Neuroimage 22 (2004) 932–940.
[28] D.H. Zald, The human amygdala and the emotional evaluation of sensory stimuli, Brain Res. Rev. 41 (2003) 88–123.
[29] Y. Zhang, J.M. Liang, W. Qin, P. Liu, K.M.V. Deneen, P. Chen, L.J. Bai, J. Tian, Y.J. Liu, Comparison of visual cortical activations induced by electro-acupuncture at vision and nonvision-related acupoints, Neurosci. Lett. 458 (2009) 6–10.